# Communication: Exciton analysis in time-dependent density functional theory: How functionals shape excited-state characters

Stefanie A. Mewes, Felix Plasser, and Andreas Dreuw

Citation: The Journal of Chemical Physics **143**, 171101 (2015);
View online: https://doi.org/10.1063/1.4935178
View Table of Contents: http://aip.scitation.org/toc/jcp/143/17
Published by the American Institute of Physics



# Communication: Exciton analysis in time-dependent density functional theory: How functionals shape excited-state characters

Stefanie A. Mewes,[1] Felix Plasser,[1,2] and Andreas Dreuw[1,a)]
[1]*Interdisciplinary Center for Scientific Computing, Ruprecht-Karls-University, Im Neuenheimer Feld 368, 69120 Heidelberg, Germany*
[2]*Institute for Theoretical Chemistry, University of Vienna, Währingstr. 17, A-1090 Wien, Austria*

(Received 7 September 2015; accepted 24 October 2015; published online 4 November 2015)

Excited-state descriptors based on the one-particle transition density matrix referring to the exciton picture have been implemented for time-dependent density functional theory. State characters such as local, extended $\pi\pi^*$, Rydberg, or charge transfer can be intuitively classified by simple comparison of these descriptors. Strong effects of the choice of the exchange-correlation kernel on the physical nature of excited states can be found and decomposed in detail leading to a new perspective on functional performance and the design of new functionals. © *2015 AIP Publishing LLC.* [http://dx.doi.org/10.1063/1.4935178]

Linear-response time-dependent density functional theory (TDDFT) is certainly one of the most widely used quantum-chemical methods for excited-state calculations of medium-size and large molecules.[1–3] At the same time, the failure of TDDFT to correctly describe charge-transfer (CT) states is well-known.[4–6] Also Rydberg states, excited states of extended $\pi$-conjugated systems,[7,8] and multiply excited states[9,10] cause difficulties. To solve conceptual short-comings, great effort has been made to search for improved functionals that reliably describe CT states, and in particular, long-range corrected (LRC) functionals featuring varying amounts of non-local exchange were developed for this purpose. The first LRC functional proposed by Yanai *et al.*[11] was a Coulomb-attenuated variant of the prominent Becke-3-Lee-Yang-Parr functional[12,13] (CAM-B3LYP), which contains non-local orbital exchange from 19% at short range up to 65% at long range.

The search for tools to diagnose the failures of TDDFT in combination with different functionals is an ongoing challenge and several descriptors measuring orbital overlaps[14–16] and centroid distances[17–19] have been proposed. However, some cases like extended symmetric $\pi$-conjugated systems, e.g., acenes, cause significant but hard-to-detect errors.[7,8,20] For these systems, the overlap of the canonical orbitals is not a good predictor of the performance of TDDFT[20–23] and a more complex dynamical view has to be adopted.

In recent work,[24–27] we established a series of excited-state descriptors based on the physical picture of an exciton wavefunction, which is constructed from the one-particle transition density matrix (1TDM) (see also Refs. 28–30). Information about the spatial distributions of *electron* and *hole* over the molecular system as well as statistical descriptors provide a solid basis for analyzing excited states. This opens a route to assign excited-state characters without the need for orbital inspection, which is beneficial for identifying problematic cases. Furthermore, the effect of a chosen exchange-correlation (xc) functional on an excited state can be investigated in detail. High-level benchmarks are accessible as the same descriptors can be computed for any method providing 1TDMs. This allows detailed benchmarking of TDDFT results going beyond a simple comparison of energies.

The central idea of our approach is the definition of an exciton wavefunction, which is identified with the 1TDM between the ground and *I-th* excited states.[26,31] In TDDFT, the 1TDM is usually constructed from the excitation and de-excitation amplitudes $X_{ia}^I$ and $Y_{ia}^I$ using the form

$$\chi_{exc}(r_h, r_e) = \sum_i^{occ} \sum_a^{virt} \left[ X_{ia}^I \phi_i(r_h) \phi_a(r_e) + Y_{ia}^I \phi_a(r_h) \phi_i(r_e) \right], \tag{1}$$

where $\phi_i$ and $\phi_a$ are the occupied and virtual molecular orbitals and $r_h$ and $r_e$ denote the coordinates of the *electron* and *hole* quasi-particles. The form of Eq. (1) is used in the current implementation, but we note for completeness that this is not a rigorous assignment as wavefunctions do not exist in TDDFT, and a different formalism suggests the use of additional scaling factors.[2,32,33] In the case of the Tamm-Dancoff approximation (TDA),[34] the same formalism is applied with the exception that the $Y_{ia}^I$ terms vanish.

Properties of the exciton wavefunction can be directly calculated as operator expectation values

$$\langle \hat{O} \rangle = \frac{\langle \chi_{exc} | \hat{O} | \chi_{exc} \rangle}{\langle \chi_{exc} | \chi_{exc} \rangle} \tag{2}$$

for any operator $\hat{O}$, whose matrix elements in the underlying orbital basis are available. The properties and relation of these expectation values to natural transition orbital analysis[35] have been discussed in detail recently.[27]

The main focus of this study is the description of spatial distributions and correlation effects of exciton wavefunctions,

a)Electronic mail: dreuw@uni-heidelberg.de; http://www.iwr.uni-heidelberg.de/groups/compchem/.

 

a task which can be achieved by computing multipole moments of the *electron* and *hole* position operators.[27] Two measures of charge transfer are investigated: the mean

$$d_{h\to e} = |\langle \vec{x}_e - \vec{x}_h \rangle| = |\langle \vec{x}_e \rangle - \langle \vec{x}_h \rangle| \tag{3}$$

and root-mean-square (rms)

$$d_{exc} = \sqrt{\langle |\vec{x}_e - \vec{x}_h|^2 \rangle} \tag{4}$$

*electron-hole* separations. While the first is a simple distance of the charge centroids, the second also includes dynamic charge separation contributions and we refer to it as exciton size. The two quantities are related by[27]

$$d_{exc}^2 = d_{h\to e}^2 + \sigma_h^2 + \sigma_e^2 - 2 \times \mathrm{COV}, \tag{5}$$

where $\sigma_h$ and $\sigma_e$ are the rms sizes of the *hole* and *electron* distributions and

$$\mathrm{COV} = \langle \vec{x}_h \cdot \vec{x}_e \rangle - \langle \vec{x}_h \rangle \cdot \langle \vec{x}_e \rangle \tag{6}$$

marks the covariance between the quasi-particles. It also follows that

$$d_{exc} \geq d_{h\to e}. \tag{7}$$

While these descriptors bear some resemblance to previous charge-transfer measures,[17,18] they stand out due to their well-defined physical meaning in the exciton picture. Furthermore, the lack of any explicit dependence on the orbitals avoids the problem of choosing the optimal representation of the orbitals in invariant subspaces.[23,36]

A recently introduced idea[27] is to quantify correlation effects between *electron* and *hole* in analogy to the Pearson correlation coefficient

$$R_{eh} = \frac{\langle \vec{x}_h \cdot \vec{x}_e \rangle - \langle \vec{x}_h \rangle \cdot \langle \vec{x}_e \rangle}{\sigma_h \sigma_e} \tag{8}$$

obtained as the normed covariance of the *electron-hole* distribution ranging from −1 to 1. A negative correlation corresponds to the picture of two charges avoiding each other dynamically. A value of zero indicates no linear correlation, i.e., *electron* and *hole* "move" independently, which is typically taken for granted when a state is analyzed with respect to molecular orbitals. Positive correlation means a joint *electron-hole* motion which can be thought of as a bound exciton. All presented excited-state descriptors are implemented in the Q-Chem 4.3 release version.

We will first examine the relation between rms exciton sizes $d_{exc}$ and charge centroid distances $d_{h\to e}$ for Tozer's benchmark set[14] as presented in Fig. 1. In these and all following computations, three functionals of different classes are applied: PBE[37] is employed as a representative of the generalized gradient approximation (GGA), B3LYP[12,13] as hybrid, and CAM-B3LYP as long-range corrected functional. The exciton descriptors are plotted against the error in excitation energy compared to experimental data, where the same geometries, basis sets, and reference data are used as in Ref. 14. Starting with exciton sizes computed by TDA/PBE, four different groups can be identified. First, locally excited states with well-described excitation energies and

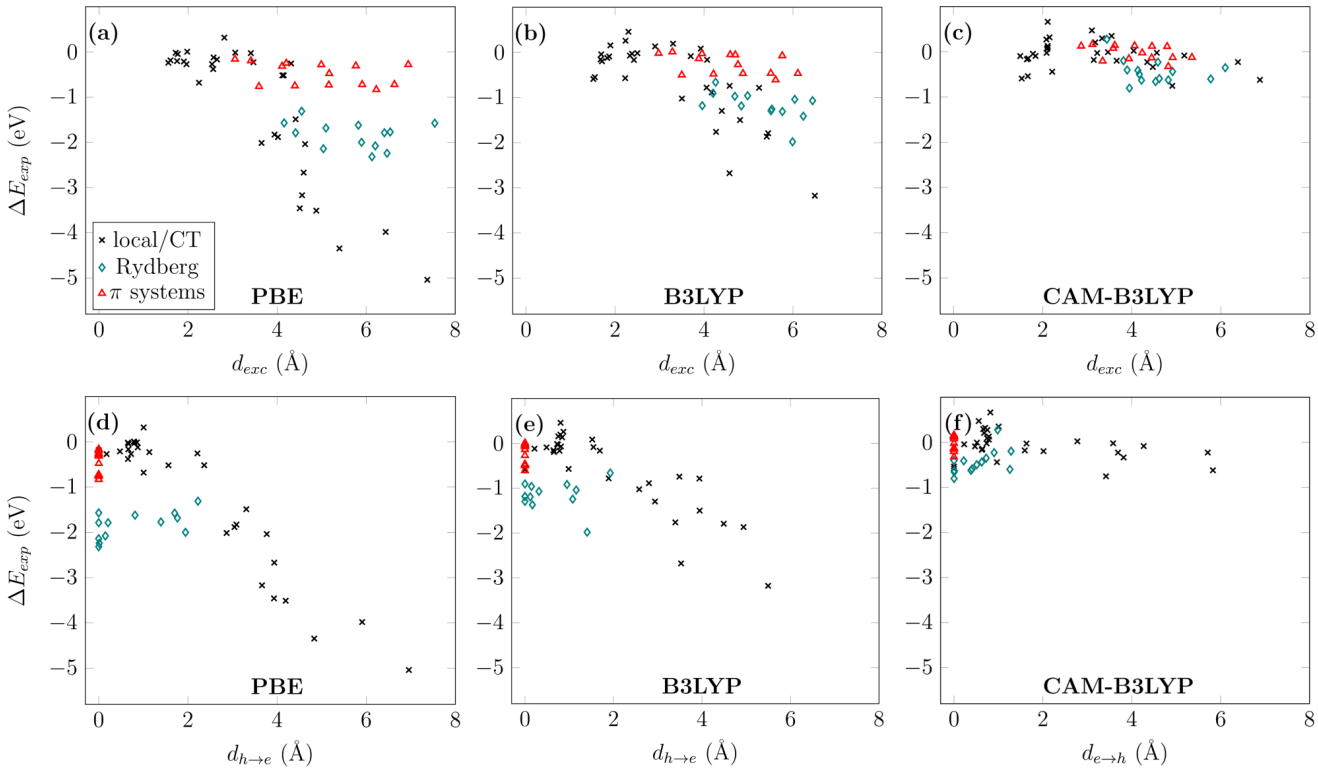


FIG. 1. Exciton sizes ($d_{exc}$, Å, first row) and center-of-mass *electron-hole* distances ($d_{h\to e}$, Å, second row) for Tozer's benchmark set[14] plotted against the error of excitation energy compared to experimental data ($\Delta E_{exp}$, eV). All presented states are singlet excited states and the Tamm-Dancoff approximation was applied. Excited states with local or directed charge-transfer character are marked in black (×), states for extended π systems (polyacenes and polyenes) in red (△), and Rydberg states in blue (◇).

small exciton sizes appear in the upper left corner of Fig. 1(a) marked in black. Second on the main diagonal, charge-transfer states with strongly underestimated excitation energies are found, where the error in excitation energies seems to scale linearly with the exciton size (also marked in black). To highlight some notoriously difficult cases, the exciton sizes for acenes and polyacetylenes are marked in red. As their energies are rather well-described using the Tamm-Dancoff approximation,[38] they appear at small deviations in $\Delta E_{exp}$ but possess large exciton sizes with a linear dependency between molecular size and exciton size. In addition, the Rydberg states are marked in blue. They have rather large exciton sizes due to their diffuse electron sizes $\sigma_e$. At the same time, their description is somewhat poorer compared to the previous group and they show a systematic underestimation of excitation energies on the order of 2 eV.

Going to the charge centroid separation $d_{h\to e}$ plotted in Fig. 1(d), the overall distribution of the black data group is preserved. The interpretation of this finding is simple: Locally excited states show only small *electron-hole* separations, however, some values above zero may occur as in some cases charges are promoted between adjacent functional groups. For the charge-transfer states, the values of $d_{h\to e}$ and $d_{exc}$ are quite similar as expected from Eq. (5) in the case for insignificant electron and hole sizes, as well as correlation effects. For the two other groups, the large conjugated systems and the Rydberg states, the situation differs dramatically. With a few exceptions for some Rydberg states, the static *electron-hole* separation $d_{h\to e}$ is zero, which means that no static charge transfer occurs. In particular in extended $\pi$ systems, an almost equal and symmetric distribution of *electron* and *hole* densities over the excited molecules and a superposition of their centroids is present. The spatial extent of the charge clouds, as measured by $\sigma_h$ and $\sigma_e$, and correlation effects are responsible for the large exciton sizes. In contrast for the Rydberg states, the dominant factor for large exciton sizes is clearly the *electron* size $\sigma_e$.

Proceeding to the B3LYP functional, locally excited states show similar exciton sizes compared to PBE. In contrast, the other states show in average a shift to smaller exciton sizes, especially in the cases of extended $\pi$ systems and Rydberg states. While the huge errors of the directed charge-transfer states are attenuated at this level, there is only a slight improvement for the extended $\pi$ system states. For the Rydberg states, the excitation energies are substantially corrected by about +1 eV compared to PBE.

For the CAM-B3LYP functional, the best performance in excitation energies is found, see Fig. 1(c). Examining the exciton sizes of the locally excited states, we find their sizes to be preserved independent of the functional choice. This comes along with almost constant excitation energy shifts with respect to experiment. In contrast, as observed before in the case of B3LYP, the states for extended $\pi$ systems and Rydberg states have a tendency to significantly smaller exciton sizes compared to PBE. To better understand this localization effect, it is worth revisiting Eq. (5). Especially for the cases where $d_{h\to e}$ is zero, the exciton size depends on the sizes of *electron* $\sigma_e$ and *hole* $\sigma_h$ and their covariance. Going from PBE to B3LYP to CAM-B3LYP for these states, a general trend is that $\sigma_{e,\mathrm{PBE}} > \sigma_{e,\mathrm{B3LYP}} > \sigma_{e,\mathrm{CAM-B3LYP}}$ and the same is observed for $\sigma_h$ which is logical considering that a diminished self-interaction error results in more compact *electron-hole* distributions. However, the variations in $\sigma_h$ and $\sigma_e$ only explain a small part of the variations in $d_{exc}$ and the covariance becomes the decisive factor for explaining the differences between the functionals. In the case of a positive *electron-hole* correlation, the resulting attraction leads to an additional compression of $d_{exc}$. In contrast for a negative correlation, the exciton size is enlarged because of the effective repulsion and charge avoidance. To gain deeper insight into this effect, the correlation coefficient $R_{eh}$ will be discussed for acenes.

We will now examine the linear *electron-hole* correlation effects with respect to the choice of functionals and compare standard linear-response TDDFT with the Tamm-Dancoff approximation. The $^1L_a$ and $^1L_b$ states of acenes from naphthalene to hexacene are calculated at the TDDFT/cc-pVTZ and TDA/cc-pVTZ levels of theory employing the PBE, B3LYP, and CAM-B3LYP functionals and the correlation coefficient $R_{eh}$ is plotted against the system size (Fig. 2). First, the $^1L_a$ states are discussed (Fig. 2(a)). For the TDDFT results indicated by solid lines, the correlation coefficient $R_{eh}$ for the PBE functional (blue) is the smallest for all molecules ranging between −0.20 and −0.15 with a trend to lower values for larger systems. This behaviour can be interpreted with the picture of two charges avoiding each other dynamically. Going to B3LYP (green), the values of $R_{eh}$ become closer to zero staying slightly below −0.05 and are almost constant for the systems larger than naphthalene. Finally, in the case of CAM-B3LYP (red) the correlation coefficient starts from approximately zero and constantly increases for larger systems to a value of 0.08 for hexacene. This positive correlation can be understood as the onset of exciton binding. This result sheds new light on the

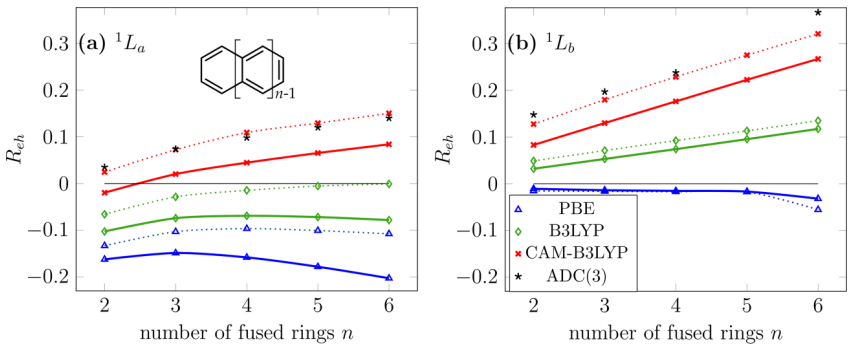


FIG. 2. Correlation coefficients $R_{eh}$ for (a) $^1L_a$ and (b) $^1L_b$ states for the acene series from naphthalene ($n = 2$) to hexacene ($n = 6$) calculated at the TDDFT/cc-pVTZ (solid lines) and TDA/cc-pVTZ (dotted lines) levels of theory employing the PBE, B3LYP, and CAM-B3LYP functionals and ADC(3)/SV(P) reference values.

observations by Tretiak *et al.*[39] that bound excitons in large conjugated systems can only be described by LRC functionals.

Going from TDDFT to TDA (dotted lines), the *electron-hole* correlation behaviour is significantly altered in favour of a stronger *electron-hole* attraction or at least a decrease of their repulsion. In the case of PBE, the average shift is about +0.06 still containing significant amount of dynamic *electron-hole* repulsion. For the B3LYP functional, an increase of $R_{eh}$ from clearly negative values of −0.05 for naphthalene to zero correlation for tetracene and larger molecules is found. This zero correlation is considered as linearly independent dynamical motion of *electron* and *hole* which is the standard assumption when inspecting molecular orbitals. Going to the long-range corrected CAM-B3LYP functional, the positive correlation increases almost constantly for all systems and ranges between 0.02 and 0.15 which is significantly higher than for TDDFT.

The values for the $^1L_b$ states are shown in Fig. 2(b) and again we will start the discussion with the TDDFT results. For PBE, the $R_{eh}$ values are approximately zero for all systems independent of their sizes. In contrast, for B3LYP and CAM-B3LYP, positive values are found with a constant increase for larger system sizes. At the same time for CAM-B3LYP, the slope of the curve is larger and a stronger trend towards bound excitons is encountered. Going to the TDA results, essentially the same trends can be observed for all functionals. However, an almost constant shift towards higher correlation values is observed with a shift of +0.02 for B3LYP and an even larger shift of +0.05 for CAM-B3LYP. The $R_{eh}$ values were recomputed at the *ab initio* level using the algebraic-diagrammatic construction method for the polarization propagator to third order (ADC(3)/SV(P)),[41] showing excellent agreement with the TDA/CAM-B3LYP level.

With the knowledge of the *electron-hole* correlation within the $^1L_a$ and $^1L_b$ states, the problems encountered to calculate excitation energies for the two states at the TDDFT level can be easily explained. For the $^1L_a$ state, a long-range corrected hybrid functional is absolutely necessary to correctly describe a bound exciton. In contrast, the physically correct picture for the $^1L_b$ state emerges already for B3LYP and in the case of PBE, at least no dynamical *electron-hole* repulsion is found. This explains the increased sensitivity of the $^1L_a$ state with respect to the choice of functional.[20,38] The level of theory and the choice of the exchange-correlation functional are very critical to obtain a physically reasonable description. In this respect, there is a decisive difference between TDDFT and TDA that Peach *et al.* related to the singlet-triplet instability issue.[40,42]

In summary, a series of excited-state descriptors based on the exciton picture has been presented for TDDFT. A wealth of information about excited-state properties can be obtained such as static *electron-hole* separations, exciton sizes, and correlation coefficients. Tozer's benchmark set was studied to illustrate how states can be characterized and different types can be distinguished based on exciton descriptors. Furthermore, the dependence of exciton properties with respect to the choice of xc-functionals can be analyzed in detail. The correlation coefficient has proven to be a powerful descriptor for the emerging *electron-hole* picture of an excited state as shown for acenes. The erroneous description of excitation energies for PBE is associated with repulsive *electron-hole* interactions. In contrast for the long-range corrected CAM-B3LYP functional, not only much better excitation energies are obtained but also particularly bound excitonic states with attractive *electron-hole* interactions are present. This effect is even enlarged when the TDA is applied and the poorer results from full TDDFT can be traced back to more weakly bound *electron-hole* pairs.

We are convinced that this detailed decomposition of exciton-related properties will further our understanding of the performance of xc-functionals in TDDFT. The methodology presented should not only be suitable for diagnosing methodological shortcomings but should, ultimately, also provide a new viewpoint for generating improved functionals. Due to the general formulation used, the quantities are also accessible in an *ab-initio* context[26,27] offering new ways for benchmarking. Finally, the computed excited-state properties open a new route for property-based diabatization schemes.[43–45]

S.A.M. acknowledges funding of the Heidelberg Graduate School of Mathematical and Computational Methods for the Sciences and Landesgraduiertenförderung Baden-Württemberg. F.P. acknowledges funding of the Alexander-von-Humboldt-Stiftung and the Vienna Scientific Cluster research school.

[1]E. Runge and E. K. U. Gross, Phys. Rev. Lett. **52**, 977 (1984).
[2]M. E. Casida, in *Recent Advances in Density Functional Methods Part I*, edited by D. P. Chong (World Scientific, Singapore, 1995), pp. 155–192.
[3]A. Dreuw and M. Head-Gordon, Chem. Rev. **105**, 4009 (2005).
[4]A. Dreuw and M. Head-Gordon, J. Am. Chem. Soc. **126**, 4007 (2004).
[5]R. J. Magyar and S. Tretiak, J. Chem. Theory Comput. **3**, 976 (2007).
[6]A. Dreuw, J. L. Weisman, and M. Head-Gordon, J. Chem. Phys. **119**, 2943 (2003).
[7]Z. L. Cai, K. Sendt, and J. R. Reimers, J. Chem. Phys. **117**, 5543 (2002).
[8]S. Grimme and M. Parac, ChemPhysChem **4**, 292 (2003).
[9]R. J. Cave, F. Zhang, N. T. Maitra, and K. Burke, Chem. Phys. Lett. **389**, 39 (2004).
[10]N. T. Maitra, F. Zhang, R. J. Cave, and K. Burke, J. Chem. Phys. **120**, 5932 (2004).
[11]T. Yanai, D. P. Tew, and N. C. Handy, Chem. Phys. Lett. **393**, 51 (2004).
[12]A. D. Becke, J. Chem. Phys. **98**, 5648 (1993).
[13]C. Lee, W. Yang, and R. G. Parr, Phys. Rev. B **37**, 785 (1988).
[14]M. J. G. Peach, P. Benfield, T. Helgaker, and D. J. Tozer, J. Chem. Phys. **128**, 044118 (2008).
[15]T. Le Bahers, C. Adamo, and I. Ciofini, J. Chem. Theory Comput. **7**, 2498 (2011).
[16]C. A. Guido, P. Cortona, B. Mennucci, and C. Adamo, J. Chem. Theory Comput. **9**, 3118 (2013).
[17]C. A. Guido, P. Cortona, and C. Adamo, J. Chem. Phys. **140**, 104101 (2014).
[18]H. Ma, T. Qin, and A. Troisi, J. Chem. Theory Comput. **10**, 1272 (2014).
[19]T. Etienne, X. Assfeld, and A. Monari, J. Chem. Theory Comput. **10**, 3896 (2014).
[20]R. Richard and J. Herbert, J. Chem. Theory Comput. **7**, 1296 (2011).
[21]B. M. Wong and T. H. Hsieh, J. Chem. Theory Comput. **6**, 3704 (2010).
[22]N. Kuritz, T. Stein, R. Baer, and L. Kronik, J. Chem. Theory Comput. **7**, 2408 (2011).
[23]B. Moore, H. Sun, N. Govind, K. Kowalski, and J. Autschbach, J. Chem. Theory Comput. **11**, 3305 (2015).
[24]F. Plasser, M. Wormit, and A. Dreuw, J. Chem. Phys. **141**, 024106 (2014).
[25]F. Plasser, S. Bäppler, M. Wormit, and A. Dreuw, J. Chem. Phys. **141**, 024107 (2014).
[26]S. A. Bäppler, F. Plasser, M. Wormit, and A. Dreuw, Phys. Rev. A **90**, 052521 (2014).
[27]F. Plasser, B. Thomitzni, S. A. Bäppler, J. Wenzel, D. R. Rehn, M. Wormit, and A. Dreuw, J. Comput. Chem. **36**, 1609 (2015).
[28]S. Tretiak and S. Mukamel, Chem. Rev. **102**, 3171 (2002).
[29]A. V. Luzanov and O. A. Zhikol, Int. J. Quantum Chem. **110**, 902 (2010).

[30]F. Plasser and H. Lischka, J. Chem. Theory Comput. **8**, 2777 (2012).
[31]M. Rohlfing and S. G. Louie, Phys. Rev. B **62**, 4927 (2000).
[32]B. F. E. Curchod, U. Rothlisberger, and I. Tavernelli, ChemPhysChem **14**, 1314 (2013).
[33]F. Plasser, R. Crespo-Otero, M. Pederzoli, J. Pittner, H. Lischka, and M. Barbatti, J. Chem. Theory Comput. **10**, 1395 (2014).
[34]S. Hirata and M. Head-Gordon, Chem. Phys. Lett. **314**, 291 (1999).
[35]R. L. Martin, J. Chem. Phys. **118**, 4775 (2003).
[36]S. Sharifzadeh, P. Darancet, L. Kronik, and J. B. Neaton, J. Phys. Chem. Lett. **4**, 2197 (2013).
[37]J. P. Perdew, K. Burke, and M. Ernzerhof, Phys. Rev. Lett. **77**, 3865 (1996).
[38]Y.-L. Wang and G.-S. Wu, Int. J. Quantum Chem. **108**, 430 (2008).
[39]S. Tretiak, K. Igumenshchev, and V. Chernyak, Phys. Rev. B **71**, 033201 (2005).
[40]M. J. G. Peach, M. J. Williamson, and D. J. Tozer, J. Chem. Theory Comput. **7**, 3578 (2011).
[41]P. H. P. Harbach, M. Wormit, and A. Dreuw, J. Chem. Phys. **141**, 064113 (2014).
[42]M. J. G. Peach, N. Warner, and D. J. Tozer, Mol. Phys. **111**, 1271 (2013).
[43]A. A. Voityuk, J. Chem. Phys. **140**, 244117 (2014).
[44]J. R. Reimers, L. K. McKemmish, R. H. McKenzie, and N. S. Hush, Phys. Chem. Chem. Phys. **17**, 24598 (2015).
[45]W. Liu, B. Lunkenheimer, V. Settels, B. Engels, R. F. Fink, and A. Köhn, J. Chem. Phys. **143**, 084106 (2015).